Thermal Stability and High-Temperature Carbon Dioxide Sorption on Hexa-lithium Zirconate ($Li_6Zr_2O_7$)

Heriberto Pfeiffer* and Pedro Bosch

Instituto de Investigaciones en Materiales, Universidad Nacional Autónoma de México, Circuito exterior s/n, Ciudad Universitaria, Apartado postal 70-360, Coyoacán, CP 04510, México, D.F., Mexico

Received December 3, 2004. Revised Manuscript Received February 4, 2005

Lithium zirconates, Li_2ZrO_3 and $Li_6Zr_2O_7$, were synthesized by solid-state reaction. The thermal analyses of $Li_6Zr_2O_7$ showed a continuous decomposition process due to lithium sublimation. However, the thermal behavior of this compound changed slightly when different gas environments were used. If nitrogen was used, $Li_6Zr_2O_7$ decomposed in a mixture of Li_2ZrO_3, ZrO_2, and $Li_2O_{(g)}$. Nevertheless, air environment produced a different and more complex decomposition mechanism at high temperatures. In this case, lithium reacted with the oxygen from the air to produce Li_2O at the surface, producing a temporary increase of the total weight. Subsequently, Li_2O and some oxygen, from the $Li_6Zr_2O_7$ structure, sublimed to produce Li_2ZrO_3 and ZrO_2. The CO_2 absorption capacity of both zirconates was studied. The materials absorbed CO_2 at around the same temperature, 450−650 °C. Still, $Li_6Zr_2O_7$ absorbed 4 times more CO_2 than Li_2ZrO_3. Furthermore, the CO_2 sorption rate of Li_2ZrO_3 was much slower than that of $Li_6Zr_2O_7$ at short times. Apparently, at the beginning of the absorption process, there was more lithium available to react with CO_2 in the $Li_6Zr_2O_7$ sample, as expected, although the sorption rates of both ceramics became similar after long times. A correlation is established between the lithium and CO_2 diffusion through the Li_2CO_3 produced on the surface of the particles. The best temperature for the CO_2 absorption on $Li_6Zr_2O_7$ was 550 °C. Finally, XRD analyses, after the CO_2 absorption, and cyclic thermogravimetric analyses showed that $Li_6Zr_2O_7$ was not regenerated. In all cases, the final product was Li_2ZrO_3.

Introduction

Carbon dioxide (CO_2) is produced in many industrial applications such as power generation by burning coal. This kind of emission has to be controlled to have a cleaner environment.[1,2] The presence of CO_2 in the environment has indeed increased the heat trapping capability of the earth's atmosphere via the greenhouse effect.[3,4] The key for the sequestration of CO_2 is to separate it from the flue gas. However, there are usually two different kinds of problems. First, N_2 and CO_2 are two of the main compounds produced in almost any flue gas, and these two compounds have similar sizes. The separation is then not easy at all. The second problem is that the flue gas is produced usually at high temperatures. Hence, the gas has to be cooled before any separation treatment.[5,6]

Nowadays, zeolites and other chemical absorbents, such as some perovskite oxides, lithium hydroxide (LiOH), and soda lime, are used as CO_2 absorbents.[7,8] Nevertheless, the capacity to absorb CO_2 in zeolites is poor, and the chemical absorbents are nonregenerable products. Hence, to find novel and more effective technologies for separation and capture of CO_2, new materials must cover the following points: (1) high selectivity and sorption capacity for CO_2 at elevated temperatures, (2) adequate absorption/desorption kinetics for CO_2, (3) good cyclability for the absorption/desorption process, and (4) good hydrothermal and mechanical properties.[3,9]

However, lithium ceramics are key components in different fields. For example, they are involved in the production of energy. Some of these ceramics are used in lithium-ion batteries, while others are candidate materials for the production of tritium into the nuclear fusion reactors.[10−14] However, a new application for lithium ceramics has been proposed recently. Lithium meta-zirconate (Li_2ZrO_3)[2,5,6,15−17] and lithium ortho-silicate (Li_4SiO_4)[1,8] seem to present CO_2 absorption features at high temperatures.

* To whom correspondence should be addressed. Phone: +52 (55) 5622 4641. Fax: +52 (55) 5616 1371. E-mail: pfeiffer@zinalco.iimatercu.unam.mx

(1) Kato, M.; Yoshikawa, S.; Nakagawa, K. *J. Mater. Sci. Lett*. **2002**, *21*, 485−487.
(2) Ida, J. I.; Xiong, R.; Lin, Y. S. *Sep. Purif. Technol*. **2004**, *36*, 41−51.
(3) Hutson, N. D.; Speakman, S. A.; Payzant, E. A. *Chem. Mater*. **2004**, *16*, 4135−4143.
(4) Hwang, C. S.; Wang, N. C. *Mater. Chem. Phys*. **2004**, *88*, 258−263.
(5) Ida, J. I.; Lin, Y. S. *Environ. Sci. Technol*. **2003**, *37*, 1999−2004.
(6) Xiong, R.; Ida, J. I.; Lin, Y. S. *Chem. Eng. Sci*. **2003**, *58*, 4377−4385.
(7) Nomura, K.; Tokumistu, K.; Hayakawa, T.; Homonnay, Z. *J. Radioanal. Nucl. Chem*. **2000**, *246*, 69−77.
(8) Essaki, K.; Nakagawa, K.; Kato, M.; Uemoto, H. *J. Chem. Eng. Jpn.* **2004**, *37*, 772−777.
(9) Yong, Z.; Mata, V.; Rodriguez, A. E. *Sep. Purif. Technol*. **2002**, *26*, 195−205.
(10) Pfeiffer, H.; Bosch, P.; Bulbulian, S. *J. Nucl. Mater*. **1998**, *257*, 309−317.
(11) Pfeiffer, H.; Knowles, K. M. *J. Eur. Ceram. Soc*. **2004**, *24*, 2433−2443.
(12) Vincent, C. A. *Solid State Ionics* **2000**, *134*, 159−167.
(13) Dell, R. M. *Solid State Ionics* **2000**, *134*, 139−158.
(14) Tarascon, J. M.; Armand, M. *Nature* **2001**, *414*, 359−367.
(15) Nakagawa, K.; Ohashi, T. *J. Electrochem. Soc*. **1998**, *145*, 1344−1346.
(16) Choi, K. H.; Korai, Y.; Mocchida, I. *Chem. Lett*. **2003**, *32*, 924−925.
(17) Nair, B. N.; Yamaguchi, T.; Kawamura, H.; Nakao, S. I.; Nakagawa, K. *J. Am. Ceram. Soc*. **2004**, *87*, 68−74.

10.1021/cm047897+ CCC: $30.25
Published on Web 03/11/2005

The reaction mechanisms proposed for CO_2 absorption into Li_2ZrO_3 and Li_4SiO_4 are summarized by the following reactions:

$$Li_2ZrO_3 + CO_2 \xrightarrow{400-600\ °C} Li_2CO_3 + ZrO_2 \xrightarrow{\geq 700\ °C} Li_2ZrO_3 + CO_2 \quad (1)$$

$$Li_4SiO_4 + CO_2 \xrightarrow{400-600\ °C} Li_2CO_3 + Li_2SiO_3 \xrightarrow{\geq 700\ °C} Li_4SiO_4 + CO_2 \quad (2)$$

The advantages of this kind of sequestration are that the reaction takes place at high temperatures and it is selective. In other words, the flue gas does not have to be cooled and N_2, or any other gas, does not interfere the reaction. Furthermore, CO_2 could be extracted in a parallel procedure at higher temperatures, regenerating the lithium ceramic.

Although Li_2ZrO_3 has been extensively characterized for different applications, other lithium zirconates, such as hexalithium zirconate ($Li_6Zr_2O_7$), have not been thoughtfully studied. $Li_6Zr_2O_7$ exhibits a monoclinic crystal structure with $a = 10.445$ Å, $b = 5.989$ Å, $c = 10.20$ Å, and $\beta = 100.26°$.[18] The Li/Zr molar ratio of $Li_6Zr_2O_7$ is 1.5 times higher than that of Li_2ZrO_3. However, $Li_6Zr_2O_7$ does not seem to be as thermally stable as Li_2ZrO_3 at high temperatures. While Li_2ZrO_3 is stable up to 900 °C, $Li_6Zr_2O_7$ decomposes in Li_2ZrO_3 at around 700 °C.[11,19]

As was mentioned previously, $Li_6Zr_2O_7$ has 1.5 times more lithium than Li_2ZrO_3 per Zr atom. In that case, it could be possible that $Li_6Zr_2O_7$ absorbs more CO_2 than Li_2ZrO_3. The aim of this work was then to study systematically the synthesis, thermal stability, and CO_2 absorption capacity of $Li_6Zr_2O_7$.

Experimental Section

Both lithium zirconates, $Li_6Zr_2O_7$ and Li_2ZrO_3, were prepared by solid-state reaction. Different amounts of lithium carbonate (Li_2CO_3) and zirconium oxide (ZrO_2) were mixed together mechanically in an agate mortar. The Li/Zr molar ratios used for the synthesis of the lithium zirconates were 2.05/1 and 3.1/1 for Li_2ZrO_3 and $Li_6Zr_2O_7$, respectively. The powders were then heat treated at different temperatures and times. While Li_2ZrO_3 was only treated 4 h at 850 °C, $Li_6Zr_2O_7$ had to be treated at 600 °C for 16 h. Between the thermal processes, $Li_6Zr_2O_7$ powder was taken out of the furnace, pulverized, and mixed.

The samples were characterized by different techniques such as X-ray diffraction (XRD), scanning electron microscopy (SEM), and thermogravimetric analysis (TGA). The XRD patterns were obtained with a Siemens D-5000 diffractometer coupled to a Cu anode X-ray tube. The Kα wavelength was selected with a diffracted beam monochromator. Compounds were identified conventionally using the JCPDS files. The percentages of the various compounds were estimated from the total area under the most intense peak for each identified phase, having an estimated experimental error of ±3%. SEM (Stereoscan 440, Cambridge) was used to determine the particle size and morphology of the materials before and after the different thermal treatments. Finally, different thermal analyses were performed in a TA Instruments equipment. Some samples were heat treated with a heating rate of 5 °C min^{-1} from room temperature to 1000 °C. These analyses were carried out under different atmospheres: air, N_2, and CO_2. However, other samples were analyzed isothermically at 450, 500, 550, 600, and 650 °C. All of the isothermal analyses were performed under an atmosphere of CO_2.

Molecular dynamics simulations were performed using the Cerius^2 software package,[20] and the $Li_6Zr_2O_7$ initial model was based on a reported structure.[18] The modules used in the Cerius^2 were the minimization and molecular dynamics modules. A supercell of $3 \times 3 \times 3$ was built to perform the molecular dynamics simulations. The $Li_6Zr_2O_7$ system consisted of 1620 particles of which 648 particles correspond to lithium atoms, 216 particles correspond to zirconium atoms, and 756 particles correspond to oxygen atoms.

Simulations were performed between 100 and 1000 °C, at steps of 100 °C. Energy was minimized on all models, before the molecular dynamics simulations, to reduce strain. Molecular dynamics simulations were performed in a micro canonical ensemble. The system was fitted to have constant volume and pressure, and it was under periodic conditions. The simulations followed two stages: First, the equilibrium of the system and, second, the data collection. The total simulation time was 10 ps for each temperature of modeling. The first 5 ps of simulation was considered as the equilibrium period, and the second 5 ps was when the accumulation of the relevant quantities was carried out to calculate the final statistical averages.

Results and Discussion

Characterization of Lithium Zirconates. Both lithium zirconates, Li_2ZrO_3 and $Li_6Zr_2O_7$, were synthesized by solid-state reaction, and they were identified with the JCPDS files, 33-0843 and 36-0122, respectively. Both zirconates presented crystalline structures, and they were the only phases detected by XRD in each case. Furthermore, SEM micrographs of these materials presented similar morphologies. The lithium zirconate particles, which had an average particle size of ~2−5 μm, produced agglomerates. The size of the agglomerates changed with the lithium zirconate. While Li_2ZrO_3 agglomerates were around 10−30 μm, some of the $Li_6Zr_2O_7$ agglomerates seemed to be larger (50−80 μm) than those of Li_2ZrO_3. This effect must be due to the time that each sample was treated. The XRD results and SEM images can be seen in the Supporting Information.

Thermal Stability. Thermogravimetric analyses of the $Li_6Zr_2O_7$ sample in air and N_2 are shown in Figure 1. Both samples presented similar behaviors between 20 and 700 °C; they lost 1−2 wt % approximately. This weight loss may be attributed to lithium sublimation as Li_2O. There are three different reactions that describe the thermal decomposition of $Li_6Zr_2O_7$ (reactions 3−5):

$$Li_6Zr_2O_7 \rightarrow Li_2O_{(g)} + 2Li_2ZrO_3 \quad (3)$$

$$Li_6Zr_2O_7 \rightarrow 2Li_2O_{(g)} + Li_2ZrO_3 + ZrO_2 \quad (4)$$

$$Li_6Zr_2O_7 \rightarrow 3Li_2O_{(g)} + 2ZrO_2 \quad (5)$$

Each reaction corresponds to the loss of one, two, or three Li_2O, and the consequent production of Li_2ZrO_3 and/or ZrO_2.

(18) Czekalla, R.; Jeitschko, W. *Z. Anorg. Allg. Chem*. **1993**, *619*, 2038−2042.
(19) Wyers, G. P.; Cordfunke, E. H. P. *J. Nucl. Mater*. **1989**, *168*, 24−30.
(20) Cerius^2, version 4.2; Accelrys: San Diego, CA, 2001.

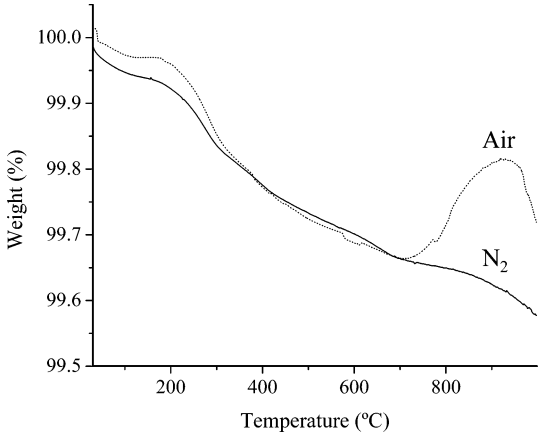

Figure 1. TGA curves of $Li_6Zr_2O_7$ analyzed under a flux of air or nitrogen.

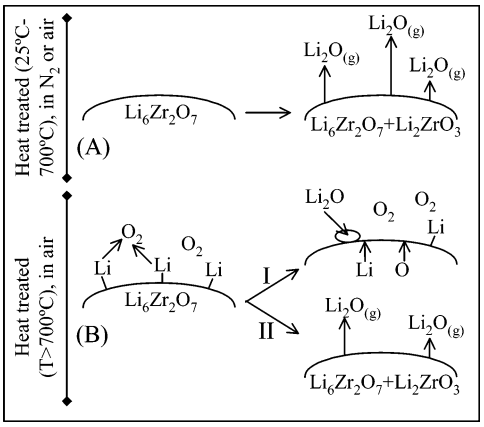

Figure 2. Scheme of two different mechanisms proposed for the thermal decomposition of $Li_6Zr_2O_7$. Mechanism A occurs at temperatures lower than 700 °C and is independent of the environment. Mechanism B is only produced in the presence of oxygen and is developed at temperatures higher than 700 °C. Processes I and II occur simultaneously. However, the kinetics of process I is faster.

At temperatures higher than 700 °C, the thermal behavior of the samples differs. While $Li_6Zr_2O_7$ heat treated in a flux of N_2 continued losing weight, the sample treated in air increased its weight. This sample gained weight between 700 and 920 °C. Finally, the weight of this sample decreased again, at temperatures higher than 940 °C. These two weight variations must be due to the presence of oxygen in the second thermogravimetric analysis.

According to reactions 3−5, $Li_6Zr_2O_7$ decomposes in Li_2O and a mixture of Li_2ZrO_3 and ZrO_2. However, at temperatures higher than 700 °C, a second and more complex mechanism of the $Li_6Zr_2O_7$ decomposition could include the reaction of lithium, present on the surface of the particles, with oxygen from the air producing Li_2O at the surface (Figure 2). This mechanism could explain the thermal behavior of the sample heat treated in air, only if the kinetics of this reaction is faster than the kinetics of Li_2O sublimation shown in reactions 3−5. Several authors have reported the vaporization and thermochemical properties of different lithium ceramics.[21−23] They have shown that the partial pressure of $Li_2O_{(g)}$ decreases in the following order: $Li_2O_{(s)} > Li_6Zr_2O_{7(s)} > Li_2ZrO_{3(s)}$. At high partial pressure of $Li_2O_{(g)}$, the sublimation process diminishes. Hence, the sublimation of $Li_2O_{(g)}$ could be blocked by the same $Li_2O_{(s)}$ produced at the surface of the particles, until the sublimation process is accelerated, while the temperature is increased. To probe this mechanism, a sample heat treated up to 850 °C in air was analyzed by XRD. A slower, detailed scan was necessary to enable the various phases to be identified (see Supporting Information). The Li_2O (220) peak was detected, confirming the existence of Li_2O. The peak (111), that is the main peak of Li_2O, could not be detected, because it over crosses with other peaks of lithium zirconates. As the Li_2O amount is very small, no significant broadening of the $Li_6Zr_2O_7$ reflections was observed.

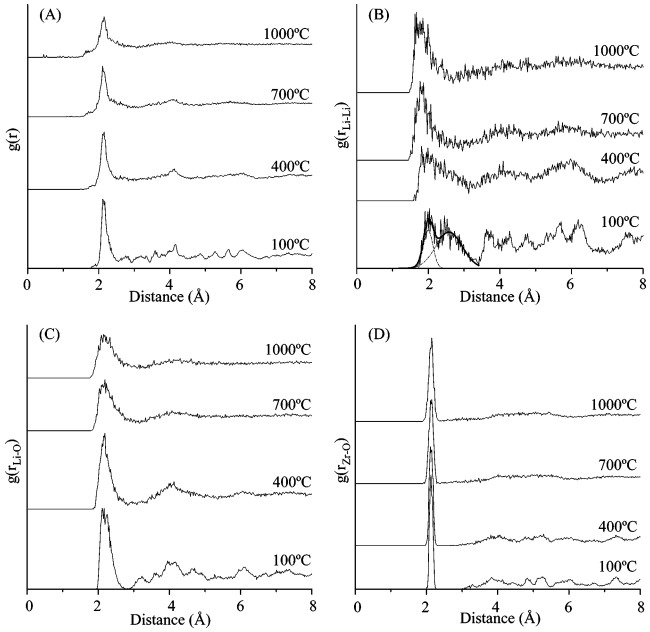

Figure 3. Theoretical radial distribution functions at 100, 400, 700, and 1000 °C for the $Li_6Zr_2O_7$ system. (A) Total radial distribution functions, (B) Li−Li partial radial distribution functions, (C) Li−O partial radial distribution functions, and (D) Zr−O partial radial distribution functions.

Furthermore, according to this mechanism, lithium diffusion, from the core of the particles through the surface, must be much faster than that of oxygen. In this way, there might be an excess of lithium on the surface that is reacting with the oxygen from the air. Molecular dynamics simulations of $Li_6Zr_2O_7$ support this hypothesis (see below).

Molecular Dynamics Simulation. The structural behavior of the studied model upon heating was analyzed. The partial radial distribution functions, $g(r)$, $g(r_{Li-Li})$, $g(r_{Li-O})$, and $g(r_{Zr-O})$, were obtained for the final structures at various temperatures (Figure 3). The total and partial distribution functions of the different pairs lose the long-range structure of the overall crystalline structure at high temperatures. The total distribution function at 100 °C presents a well-defined structure. However, at higher temperatures, the order is lost as a function of the temperature. The $g(r_{Li-Li})$ presents a double peak at 100 °C (Figure 3B). These peaks are centered at 1.99 and 2.58 Å, respectively. The peaks correspond to the two different Li−Li distances in the $Li_6Zr_2O_7$ structure. However, when the temperature is increased, these peaks are shifted to lower values. Finally, at 1000 °C, there is only

(21) Asano, M.; Kato, Y.; Harada, T.; Mizutani, Y. *J. Nucl. Mater*. **1996**, *230*, 110−115.
(22) Dash, S.; Sood, D. D.; Prasad, R. *J. Nucl. Mater*. **1996**, *228*, 83−116.
(23) Zou, Y.; Petric, A. *J. Phys. Chem. Solids* **1994**, *55*, 493−499.

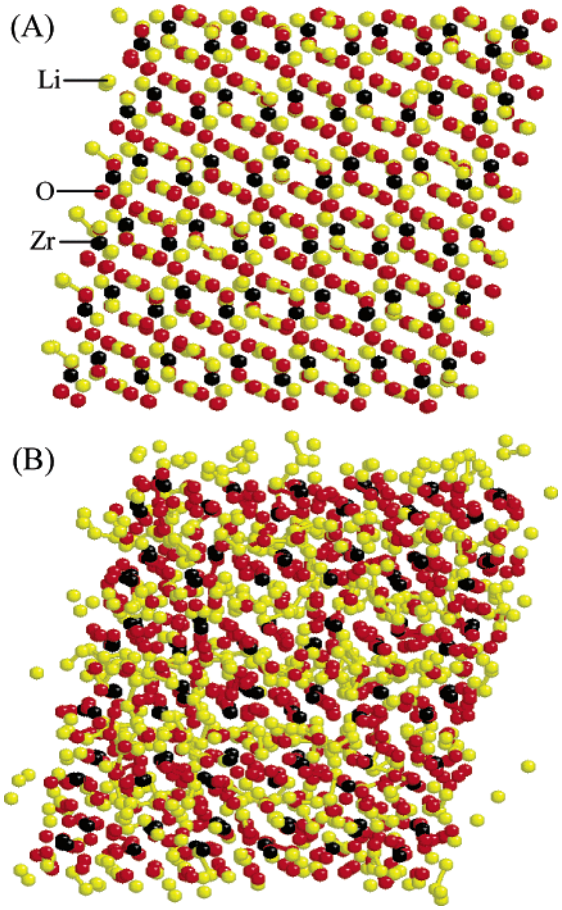

Figure 4. Snapshots of the final configuration for the $Li_6Zr_2O_7$ systems heat treated at (A) 100 °C and (B) 1000 °C. The intensity of the color in the spheres, from darker to brighter, corresponds to zirconium, oxygen, and lithium atoms, respectively.

one asymmetric peak centered at 1.84 Å. This effect can be attributed to the lithium atoms moving out of the structure. This effect must influence the change of phase detected previously, which corresponds to the decomposition process of the $Li_6Zr_2O_7$, where Li_2O is sublimated. None of the other element pairs presented this kind of behavior. In all of the cases, the short distance interactions of the different pairs were preserved, and only the long distance interactions were lost due to the decomposition process (Figure 3C and D).

Figure 4 shows snapshots of the final configurations at 100 and 1000 °C. The crystalline configuration does not vary at 100 °C (Figure 4A); actually, it is not easy to visualize the atomic movements at all. However, the snapshot of the model heat treated at 1000 °C presents a sort of amorphization (Figure 4B). Furthermore, the lithium atoms seem to diffuse to the surface of the system. Apparently, lithium atoms take up and diffuse through the internal pores, while zirconium and oxygen atoms tend to stay close to their original positions.

Figure 5 shows the self-diffusion coefficient (D) of the three elements as a function of the temperature. At low temperatures (100−600 °C), the diffusion in the crystal is poor. None of the elements, Li, Zr, or O, moves considerably at these temperatures. The crystalline structure is then preserved. However, at temperatures higher than 600 °C, the self-diffusion coefficient of lithium presents a dramatic change, if compared to the zirconium and oxygen coefficients. While the lithium coefficient increased, the coefficient of zirconium and oxygen did not change significantly. The activation energy of the Li diffusion is then reached at around 700 °C, producing the decomposition of the $Li_6Zr_2O_7$. The high diffusion of the lithium atoms represents properly the lithium sublimation as Li_2O at high temperatures, where lithium reacts with the environmental oxygen. These theoretical calculations are in excellent agreement with the TGA results, where a faster lithium diffusion was proposed into the $Li_6Zr_2O_7$ particles at temperatures equal to or higher than 700 °C.

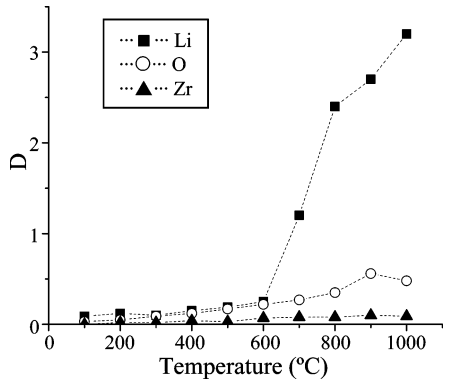

Figure 5. Self-diffusion coefficients (D) of lithium, zirconium, and oxygen atoms, as a function of temperature.

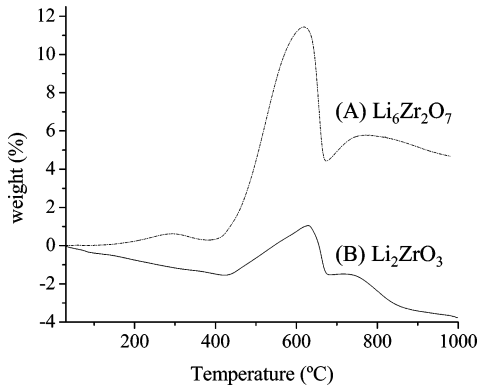

Figure 6. Thermogravimetric analyses of Li_2ZrO_3 and $Li_6Zr_2O_7$ into a flux of CO_2.

Carbon Dioxide Absorption. As Li_2ZrO_3 presents good qualities as CO_2 absorbent material, $Li_6Zr_2O_7$ was expected to present a similar or better behavior due to its higher Li/Zr molar ratio. If $Li_6Zr_2O_7$ absorbs CO_2, the following reactions may occur:

$$Li_6Zr_2O_7 + 3CO_2 \rightarrow 3Li_2CO_3 + 2ZrO_2 \quad (6)$$

$$Li_6Zr_2O_7 + 2CO_2 \rightarrow 2Li_2CO_3 + ZrO_2 + Li_2ZrO_3 \quad (7)$$

$$Li_6Zr_2O_7 + CO_2 \rightarrow Li_2CO_3 + 2Li_2ZrO_3 \quad (8)$$

For comparison purposes, Li_2ZrO_3 was used as standard. In this way, the difference in CO_2 absorption capacity, of both lithium zirconates, is clearly shown in Figure 6. Although Li_2ZrO_3 lost 2 wt % at low temperatures due to a dehydration process, both zirconates presented similar CO_2 absorption processes. Both materials absorbed CO_2 at around the same temperature, between 450 and 650 °C. Nevertheless, $Li_6Zr_2O_7$ presented an absorption higher than that of Li_2-

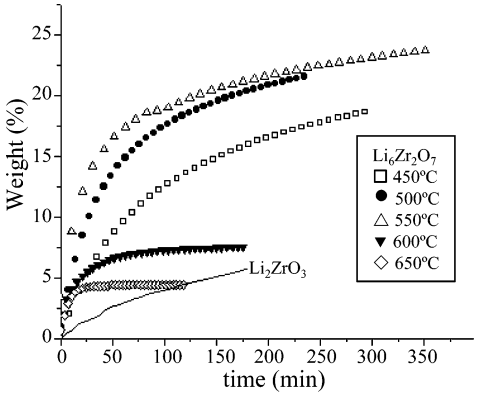

Figure 7. Isothermal analyses of Li_2ZrO_3 heat treated at 500 °C (line) and $Li_6Zr_2O_7$ heat treated at different temperatures (marks), into a flux of CO_2.

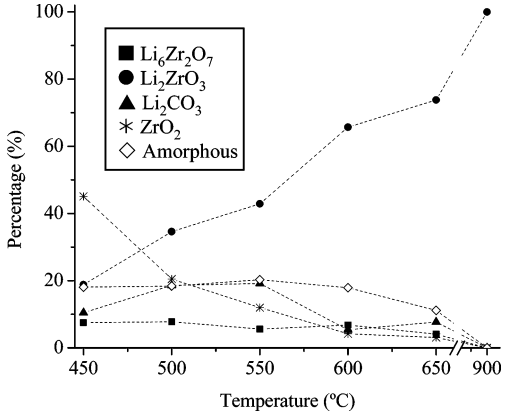

Figure 8. Final composition, as determined by XRD, of the $Li_6Zr_2O_7$ samples after the TGA into a flux of CO_2.

ZrO_3. While $Li_6Zr_2O_7$ showed a maximum weight increase of 11.4 wt %, Li_2ZrO_3 only presented a total weight increase of 2.6 wt %. The CO_2 absorption values presented by Li_2ZrO_3 are in agreement with its particle size, as previously reported by Choi et al.[16] Therefore, as the particle sizes of both zirconates were similar, the high absorption values observed for $Li_6Zr_2O_7$ are not caused by a particle size effect and are merely produced by a higher CO_2 absorption capacity.

After the absorption process, both zirconates desorbed CO_2, at around 680 °C. Finally, at temperatures higher than 700 °C, lithium zirconates presented different behaviors. $Li_6Zr_2O_7$ presented a small weight increase. It may be associated with a second absorption of CO_2. If Li_2O is produced, it could react with CO_2 producing Li_2CO_3 that disappears later by thermal decomposition. However, Li_2ZrO_3 seems to be stabilized after its regeneration, but at temperatures higher than 800 °C, it decomposes as represented in reaction 9.

$$Li_2ZrO_3 \rightarrow ZrO_2 + Li_2O_{(g)} \quad (9)$$

Figure 7 shows the isothermal graphs of Li_2ZrO_3 at 500 °C and $Li_6Zr_2O_7$ at different temperatures. While Li_2ZrO_3 absorbed only 6.3 wt % after 180 min, $Li_6Zr_2O_7$ absorbed almost 20 wt % during the same period of time. As in the TGA analysis, the CO_2 absorption of $Li_6Zr_2O_7$ was almost 4 times higher than the absorption of Li_2ZrO_3. Furthermore, at short times (between 0 and 60 min), the CO_2 sorption rate of Li_2ZrO_3 is much slower than that of $Li_6Zr_2O_7$, as shown by the slope of the curves, in the same period of time, 0.20 and 0.03 wt % min^{-1} for $Li_6Zr_2O_7$ and Li_2ZrO_3, respectively. Apparently, at the beginning of the absorption process, there are more lithium atoms available to react with CO_2 in the $Li_6Zr_2O_7$. However, the sorption rate of both zirconates becomes similar at long times due to the diffusion of lithium and carbon dioxide through the Li_2CO_3 produced over all of the surface of the particles.

The sorption rates at different temperatures presented similar behaviors as the sample treated at 500 °C and described previously, but the quantity of CO_2 absorbed changed as a function of temperature (Figure 7). When the CO_2 absorption process was performed at 450 °C, 0.192 $g_{CO2}/g_{Li6Zr2O7}$ was retained after 5 h. If the absorption process was developed at 500 and 550 °C, the amounts of absorbed CO_2 were 0.22 and 0.23 $g_{CO2}/g_{Li6Zr2O7}$, in the same period of time. However, when the absorption process was at 600 °C or higher temperatures, the CO_2 absorbed decreased dramatically to less than 0.07 $g_{CO2}/g_{Li6Zr2O7}$. Furthermore, in these samples, the equilibrium was reached after 1 h of sorption. These changes in the absorption process should be related again to the $Li_6Zr_2O_7$ decomposition process. As it was shown in the previous section, $Li_6Zr_2O_7$ decomposes in Li_2ZrO_3, according to reactions 3−5. This decomposition process must then inhibit the sorption process, and the small quantities of CO_2 absorbed may be associated with the Li_2ZrO_3 absorption process.

The composition of the $Li_6Zr_2O_7$ powders after the CO_2 isothermal absorption is summarized in Figure 8; these results were determined from the XRD patterns. Crystalline $Li_6Zr_2O_7$ almost disappeared after all of the sorption processes. The amounts of $Li_6Zr_2O_7$ were about 7−8 wt %. Even for low sorption temperatures, $Li_6Zr_2O_7$ decomposes, producing an amorphous material and other crystalline compounds. Actually, the quantity of amorphous material was ∼18 wt % in all cases. This amorphous material could be a mixture of different noncrystalline compounds such as ZrO_2, Li_2O, Li_2CO_3, and Li_2ZrO_3 produced during the CO_2 absorption and $Li_6Zr_2O_7$ decomposition processes. The Li_2CO_3 quantities detected by XRD, at the different sorption temperatures, are in excellent agreement with the isothermal absorption analysis presented previously. The maximum quantity of Li_2CO_3 was obtained for the samples treated 500 and 550 °C, 18.6 and 19.2 wt %, respectively. Instead, the quantities of ZrO_2 and Li_2ZrO_3 followed an opposite behavior. While the ZrO_2 amounts decreased, the total Li_2ZrO_3 increased, both as a function of the temperature. These changes in the composition may be correlated to the $Li_6Zr_2O_7$ decomposition and the CO_2 desorption processes. At 450 °C, the CO_2 absorption rate must be higher than the $Li_6Zr_2O_7$ decomposition process, producing more ZrO_2 according to reactions 6 and/or 7. However, at higher temperatures the $Li_6Zr_2O_7$ decomposes quickly, producing Li_2ZrO_3 and small quantities of ZrO_2 as shown by reactions 3−5. Finally, when the sample was heated to 900 °C, the only compound detected was Li_2ZrO_3, confirming that $Li_6Zr_2O_7$ decomposes to produce Li_2ZrO_3.

The morphology and particle size of the $Li_6Zr_2O_7$ after the CO_2 absorption were determined by SEM (Figure 9). None of the samples presented significant changes in

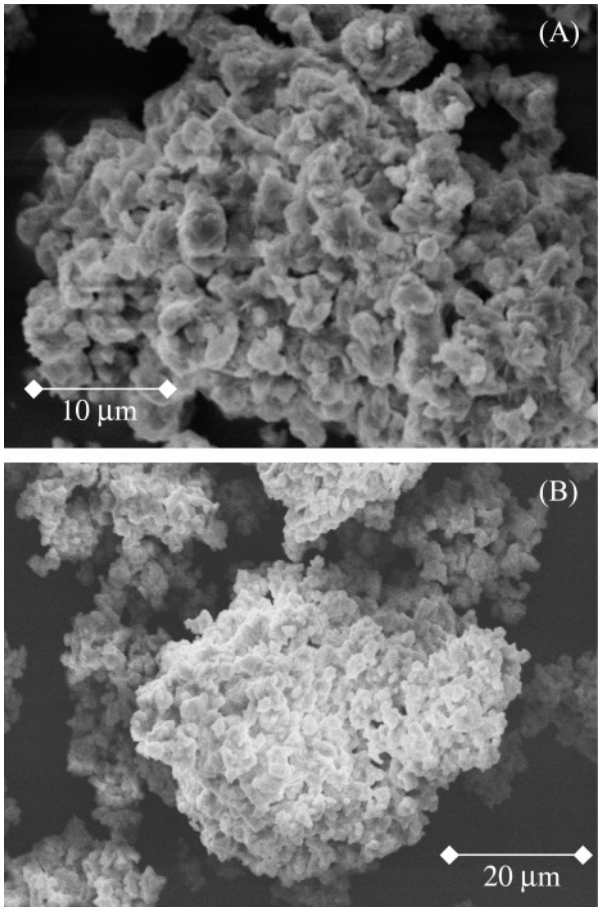

Figure 9. SEM images of $Li_6Zr_2O_7$ after thermal treatment at (A) 500 °C and (B) 900 °C into a flux of CO_2.

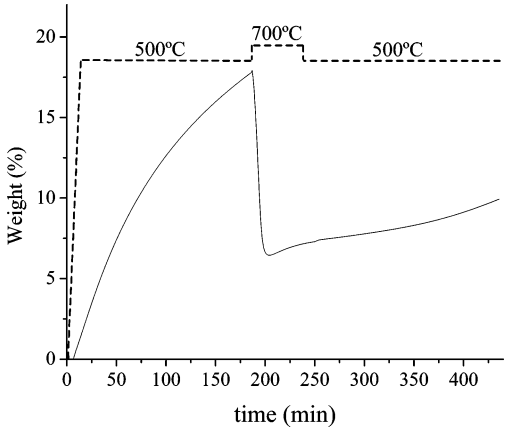

Figure 10. Cyclic thermogravimetric analysis of the CO_2 absorption and desorption processes.

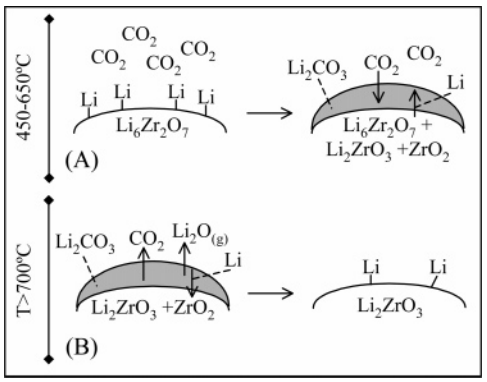

Figure 11. Schematic illustration of the carbonation and decarbonation mechanisms of $Li_6Zr_2O_7$ at high temperatures.

comparison with the same sample before any absorption process. The material remained as agglomerated particles of 3−5 μm. Perhaps, the only difference is that, now, the agglomerates seem to be denser and the particles less corrugated. These effects can be easily explained by the CO_2 absorption process, which implies the presence of more material and the change of the surface morphology.

From these results, it is possible to infer that $Li_6Zr_2O_7$ does not regenerate after the CO_2 desorption, as Li_2ZrO_3 does. The CO_2 absorption may then decrease as well after the first absorption cycle. To check this hypothesis, a cyclic thermogravimetric analysis was performed. First, $Li_6Zr_2O_7$ was treated at 500 °C for 3 h, then it was heated for 1 h at 700 °C, and finally the sample was cooled at 500 °C for 3 h again (Figure 10). In the first heat treatment, the weight increased 17.7 wt %, as expected, due to the CO_2 absorption. When the sample was heated (700 °C/1 h), the desorption process occurred immediately. However, not all of the CO_2 was desorbed; around 6.6 wt % of the initially absorbed CO_2 remained trapped into the material. Li_2ZrO_3 usually presented a total desorption of CO_2,[5] but $Li_6Zr_2O_7$ did not present the same behavior, probably due to its decomposition at lower temperatures. Hence, as a result of the $Li_6Zr_2O_7$ decomposition, during the first desorption process, the second CO_2 absorption was not efficient. Actually, in the second process, the weight increased less than 5 wt %. This second absorption has to be mainly attributed to the Li_2ZrO_3, produced through the $Li_6Zr_2O_7$ decomposition.

A summary of the CO_2 absorption mechanism on $Li_6Zr_2O_7$ is shown in Figure 11. The results clearly show that $Li_6Zr_2O_7$ absorbs CO_2 very efficiently between 450 and 600 °C. Lithium, from $Li_6Zr_2O_7$, reacts with the CO_2 to produce Li_2CO_3 at the surface of the particles. Lithium and CO_2 then have to diffuse in opposite ways, through the Li_2CO_3 core to continue reacting. This process is given by a series of reactions (reactions 6−8), where the final product is a mixture of ZrO_2, Li_2ZrO_3, and Li_2CO_3. Moreover, when this sample is heated at higher temperatures than 700 °C, Li_2CO_3 decomposes as CO_2 and lithium. In this step, lithium reacts with ZrO_2, producing Li_2ZrO_3, and another part sublimates as Li_2O.

Conclusions

The thermal stability and CO_2 absorption of $Li_6Zr_2O_7$ were investigated in this work. First, thermal analyses show that $Li_6Zr_2O_7$ decomposes continuously due to lithium sublimation as Li_2O. However, the thermal behavior changed slightly if different gas environments are used. When nitrogen is used, Li_2O is produced by a direct thermal decomposition of $Li_6Zr_2O_7$. Nevertheless, air produces a different and more complex decomposition mechanism at temperatures ≥700 °C. In this case, lithium reacts with the oxygen from the air to produce Li_2O, producing a temporary increase of the weight. Afterward, Li_2O and some oxygen from the $Li_6Zr_2O_7$ structure sublime to produce Li_2ZrO_3 and ZrO_2.

When $Li_6Zr_2O_7$ was tested, it presented a high CO_2 absorption, in comparison with the observed values for Li_2-

ZrO_3. Both materials absorb CO_2 between 450 and 600 °C, but $Li_6Zr_2O_7$ absorbs up to 4.4 times the maximum quantity absorbed by Li_2ZrO_3. The best temperature for the CO_2 absorption on $Li_6Zr_2O_7$ was 550 °C, where the CO_2 absorbed was 0.23 $g_{CO2}/g_{Li6Zr2O7}$. Furthermore, $Li_6Zr_2O_7$ absorbs CO_2 faster than Li_2ZrO_3 at short times, because there is more lithium available on the surface. Once the lithium of the surface has totally reacted and produced Li_2CO_3, the rates of absorption become similar for $Li_6Zr_2O_7$ and Li_2ZrO_3.

Different analyses such as the composition after the CO_2 absorption and cyclic thermal analyses confirm that $Li_6Zr_2O_7$ does not regenerate after the CO_2 desorption. In this case, $Li_6Zr_2O_7$ decomposes into Li_2ZrO_3.

Acknowledgment. We thank Dr. Piña for the laboratory facilities, Dr. Valladares for the computational facilities, and C. Vasquez and L. Baños for technical work in the thermal and XRD analyses, respectively.

Supporting Information Available: XRD patterns and SEM images (PDF). This material is available free of charge via the Internet at http://pubs.acs.org.

CM047897+